Full-waveform inversion of cycle-skipped seismic data by frequency down-shifting

Michael Warner, Tenice Nangoo, Nikhil Shah, Adrian Umpleby and Joanna Morgan, Imperial College London.

Summary

Full-waveform inversion can be severely compromised by problems of cycle skipping; this occurs when predicted and observed data differ by more than half a cycle, and it leads the inversion to recover a local rather than the global minimum model. Overcoming cycle skipping normally requires both a good starting model and low-frequency content in the field data. Here we present a scheme that uses a non-linear extrapolation to add missing low-frequencies into the field data. We demonstrate the scheme using a 3D OBC field dataset, and show that it can invert to recover the global minimum model even when the original un-extrapolated field dataset is significantly cycle skipped.

Introduction

Full-waveform inversion (FWI) is an optimization scheme that seeks to find the global minimum of the misfit between field seismic data and synthetic data generated by a model. It proceeds towards the global minimum by a series of local linearized iterations from a starting model. The true relationship between model and data however is non-linear, and several of these non-linearities can lead the inversion scheme to become trapped within local minima rather than reaching the desired global solution.

Amongst these non-linearities, the most important is that produced by the oscillatory nature of the seismic data themselves. A cycle-skipped starting model, that is one that produces data that differ by more than half a cycle with respect to the field data, will normally lead the inversion in entirely the wrong direction towards a local minimum. This problem is well known; its practical solution typically requires a highly accurate starting model combined with low-frequency field data. In these circumstances, the predicted starting data are not cycle skipped at the lowest frequencies, and the global solution can be found by starting FWI using the lowest frequencies in the field data.

In this paper, we present a FWI scheme that relaxes the requirement for low-frequency field data and a good starting model, and that is able to reach the global minimum solution even when the starting data are cycle skipped. We do this by using the observed field data to synthesize low-frequency data that were not present in the original field data. We then invert these invented low-frequencies, which has the effect of dragging the starting model towards the global minimum. We then switch to invert the true field data which are now no longer cycle skipped, and so reach the global minimum.

Method

The essence of our method is to take band-limited field data, and to apply a non-linear operation to it to synthesize low-frequency content that was not present in the original data. In principle there are many ways to achieve this, but we require low frequencies that are sufficiently similar to the true data that they will serve to move a poor starting model in broadly the right direction when a full-waveform inversion scheme is applied to them.

We use two wavelets: one is the band-limited wavelet actually used to acquire the field data, and the other is an extended low-frequency wavelet that we would like to substitute for the field wavelet. Effectively the latter is the wavelet that we would like to have been able to use to acquire the field data, and that our scheme will simulate. These wavelets do not include ghosts or multiples.

To produce data that are frequency down-shifted, we use a sparse L1-norm to deconvolve the true wavelet from the field data to produce traces composed of a small number of spikes, which we then convolve with the substituted wavelet. We add two enhancements – we operate on the complex trace so that the spikes have complex amplitudes, and we add an additional L2-minimisation that optimizes the amplitude of the individual spikes after the L1-optimisation has identified their temporal position.

These new data now contain low-frequencies that were not present in the original field data. These new low frequencies have a hybrid existence – they behave as genuine low-frequencies with respect to cycle skipping, but they do not properly obey the wave equation. Instead, they have spatial and amplitude properties that are related to those of the higher frequencies that were used to synthesize them – effectively they obey the wave equation at the wrong frequency. Their use in a FWI scheme that is driven by the wave equation therefore requires care.

We forward propagate the original field wavelet to generate high-frequency predicted data. We apply frequency down-shifting to both the predicted and field data at the receivers, we subtract these to produce low-frequency residuals, and we back propagate these residuals. We then cross-correlate this residual wavefield with a second forward wavefield generated using the low-frequency substituted wavelet. In this way, both the predicted and field data are treated identically, and the inversion does indeed head towards the global minimum.

DOI http://dx.doi.org/10.1190/segam2013-1067.1

Field data example

We have tested this inversion scheme on a 3D field dataset. To do this, we used data from the Tommeliten OBC survey in the North Sea. We have previously worked extensively on these data using conventional FWI, and so are able to compare our results against that experience. The field data form a conventional multi-component shallow-water ocean-bottom survey. The inversion of this dataset is described at length in Warner et al (2013); we invert only the pressure data, we retain ghosts and multiples in the field data, and use a free-surface to simulated these during FWI. The lowest useful frequencies in the field data are at about 3 Hz. Conventional FWI begins at this frequency, and the data are not cycle skipped at 3 Hz with respect to our starting model. The data are however cycle skipped over the majority of the survey area at a frequency of 6 Hz.

To demonstrate the new scheme, we first removed the low frequencies from the field data, high-pass filtering them and adding noise to mask any remnant energy below 6 Hz. Figure 1(a) shows the average power spectrum of the raw field data, and Figure 1(b) shows the power spectrum of the same data after removal of the lowest frequencies – below about 6 Hz there is only noise in the high-pass filtered dataset. Figure 2(a) shows a single shot record from one cable after high-pass filtering. Figure 2(b) shows the same shot record after complimentary low-pass filtering – these are the data that have been removed from the field record in order to produce Figure 2(a). The power spectrum corresponding to Figure 2(b) is shown in Figure 1(c).

The purpose of our inversion scheme then is to take the data from Figure 2(a), to apply frequency down-shifting to it to produce shot records that resemble Figure 2(b), and to use this down-shifted data to begin FWI, moving thereafter to conventional FWI using only the high-pass filtered data. If this inversion scheme recovers essentially the same model from the 6-Hz data as was previously obtained from the full-bandwidth 3-Hz data, then it is clear that we can use the scheme to apply FWI successfully to analogous datasets that do not contain useful data below 6 Hz.

Figure 2(c) shows a low-frequency shot record synthesized by our down-shifting algorithm. We are using a non-linear deconvolution to do this, that replaces one wavelet by another that has non-overlapping bandwidth; Wiener filters and other linear deconvolution schemes cannot achieve this. Figure 1(d) shows the corresponding power spectrum. If the scheme were perfect, then Figures 2(b) and 2(c) would be identical; clearly they are not. The key question then is whether they are sufficiently similar that the synthesized data can be used as input to FWI in order to move a poor starting model in broadly the right direction so that the resulting model is no longer cycle skipped.

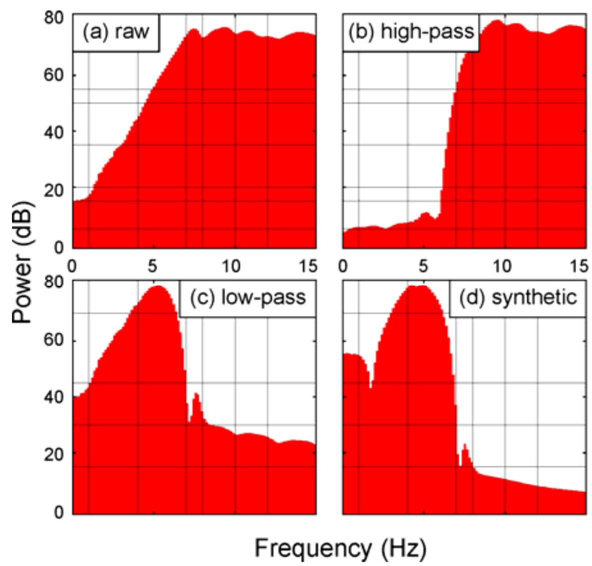

Figure 1: Average power spectra of: (a) raw field data, (b) high-pass filtered data, (c) low-pass filtered data, (d) low-pass data recovered by frequency downshifting.

Figure 3 shows horizontal depth slices through the starting velocity model, the model produced by conventional FWI applied to the cycle-skipped high-pass filtered data, the model produced by conventional FWI applied to the full-bandwidth field data, and by FWI applied to the downshifted data followed by conventional FWI applied to the high-pass filtered data. Clearly, conventional FWI fails catastrophically when the input data are cycle skipped, Figure 3(b). However, when these same cycle-skipped data are first used to synthesize down-shifted data, the resulting FWI model, Figure 3(d), closely matches the model recovered using the non-cycle-skipped full-bandwidth data.

Figures 3(c) and 3(d), while similar, differ in detail. A final test therefore is how well they depth migrate the reflection data. Figure 4 shows that the two models produce almost identical depth-migrated images, and so the differences between the two velocity models are not significant.

Conclusions

The broad application of full-waveform inversion has been limited by the necessity to acquire datasets that contain low frequencies, and by the difficulty of obtaining sufficiently accurate starting models. We have shown that it is possible to overcome both these limitations by synthesizing pseudo low-frequency data from higher frequencies, and that these down-shifted data can be used successfully for FWI when the original data are compromised by cycle skipping.

DOI http://dx.doi.org/10.1190/segam2013-1067.1

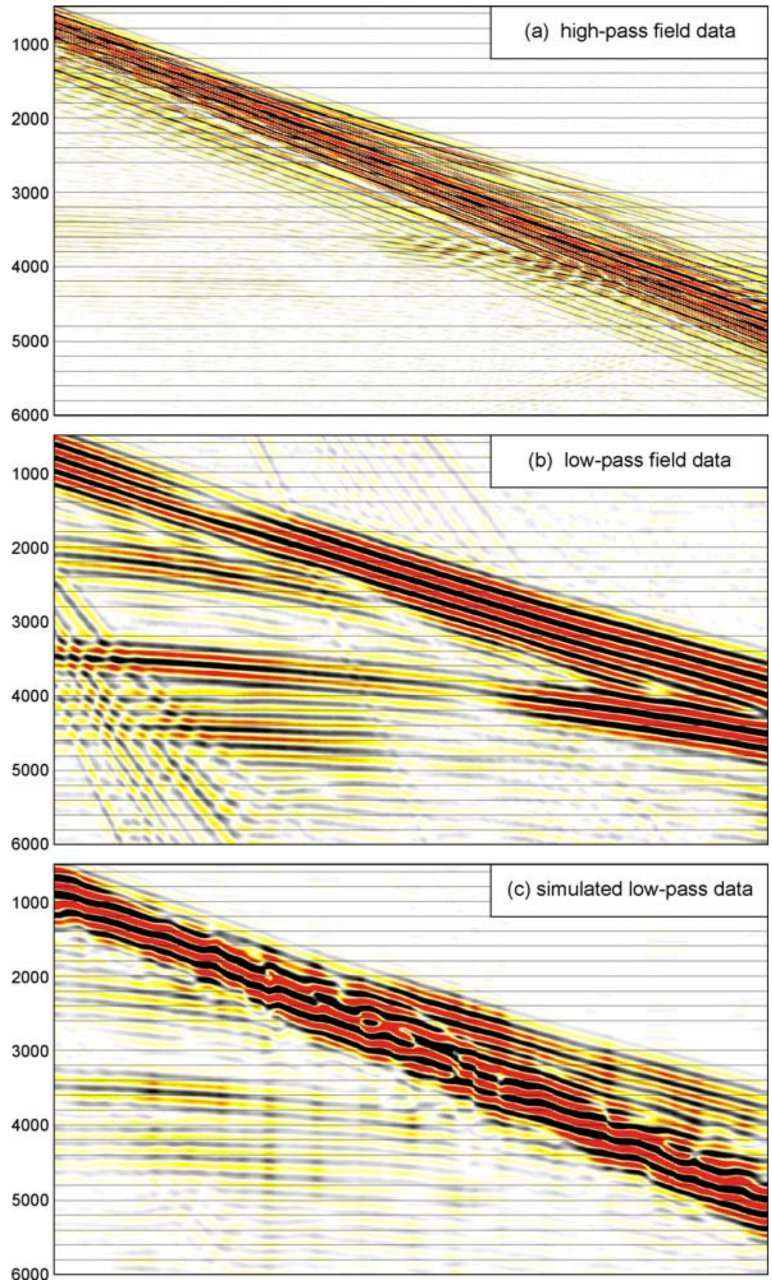

Figure 2 Shot records from the Tommeliten survey recorded on a single ocean-bottom hydrophone cable: (a) High-pass filtered above 6 Hz, (b) Low-pass filtered below 6 Hz, (c) Low-pass recovered by frequency downshifting of the high-pass filtered data. The recovered data fit the travel times of the low-pass filtered data accurately; they do not predict relative amplitudes well, and do not predict the slow Scholte waves that were not present in the input high-pass data – neither of these are used during FWI.

DOI http://dx.doi.org/10.1190/segam2013-1067.1

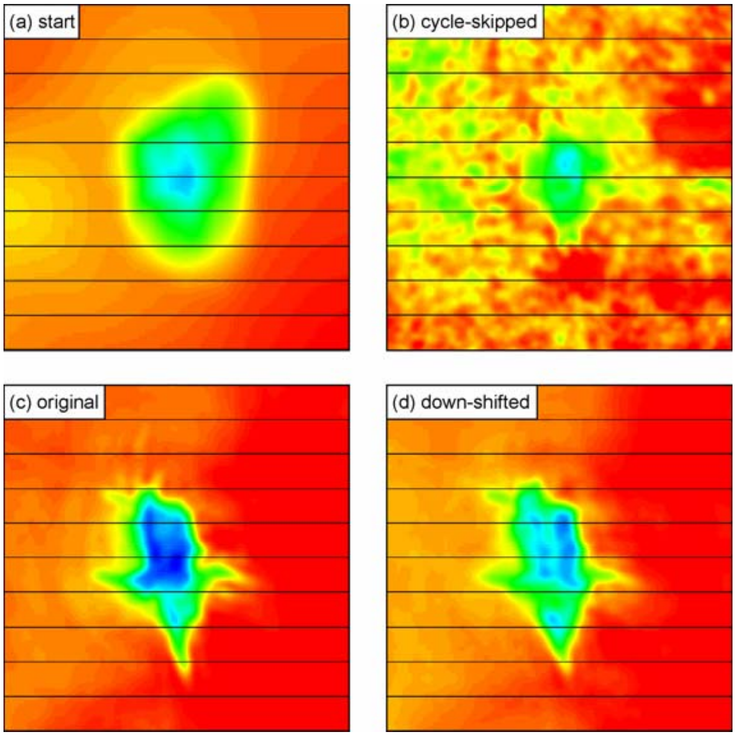

Figure 3 Horizontal slices through velocity models at a depth of 1200 m: (a) the starting model, (b) the FWI model recovered using high-pass filtered data – these data are cycle skipped and the model is nonsense, (c) the conventional FWI model, (d) the FWI model recovered by inverting the downshifted data followed by the high-pass filtered data – this model is similar to (c). The central low-velocity body is a gas cloud. Velocities range from 1600 (blue) to 2200 (red) m/s.

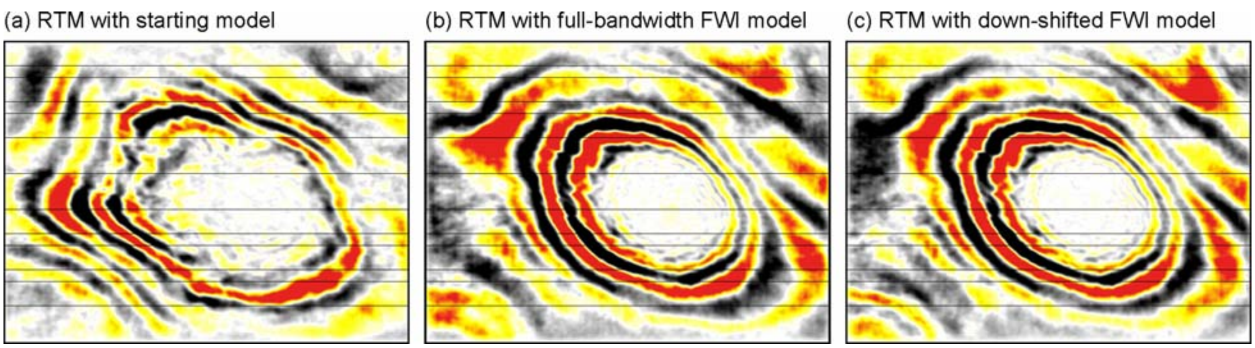

Figure 4 Horizontal slices through RTM images of the reflection data at a depth of 3600 m, migrated using (a) the starting model, (b) the conventional FWI model, (c) the FWI model recovered from down-shifted and high-pass filtered data. Both the FWI migrations simplify and sharpen the depth image, and the differences between the two FWI images are minimal.

DOI http://dx.doi.org/10.1190/segam2013-1067.1

http://dx.doi.org/10.1190/segam2013-1067.1

EDITED REFERENCES

Note: This reference list is a copy-edited version of the reference list submitted by the author. Reference lists for the 2013 SEG Technical Program Expanded Abstracts have been copy edited so that references provided with the online metadata for each paper will achieve a high degree of linking to cited sources that appear on the Web.

REFERENCES

Warner, M., A. Ratcliffe, T. Nangoo, J. Morgan, A. Umpleby, N. Shah, V. Vinje, I. Štekl, L. Guasch, C. Win, G. Conroy, and A. Bertrand, 2013, Anisotropic 3D full-waveform inversion: Geophysics, **78**, no. 2, R59–R80.